

Theoretical calculations of hyperfine interactions of the Jahn-Teller distorted single vacancy in silicon

Yong-Qiang Jia and Guo-Gang Qin

Department of Physics, Peking University, Beijing, People's Republic of China

(Received 29 June 1987)

An attempt is made to extend the theories of Hjalmanson *et al.* and Ren *et al.* for a substitutional defect in an unrelaxed sp^3 -bonded semiconductor to calculate the wave functions of electrons localized near the Jahn-Teller distorted single vacancies (positively charged vacancy V^+ and negatively charged vacancy V^-) in Si. The extent of the defect potential is firstly localized at the vacancy site in the central-cell potential approximation and then is extended to the nearest-neighbor sites considering both diagonal and off-diagonal matrix elements of the defect potential. From the calculated wave functions the hyperfine interactions of the electrons with ^{29}Si nuclei around the single vacancies (V^+ and V^-) are obtained to compare with those determined experimentally by electron paramagnetic resonance or electron-nuclear double resonance. Good agreements are obtained for the nearest-neighbor atoms of both V^+ and V^- with the central-cell potential and closer agreements with the extended potential.

I. INTRODUCTION

Both electron paramagnetic resonance (EPR) and electron-nuclear double resonance (ENDOR) are powerful tools for the study of point defects in semiconductors. From the hyperfine-interaction terms which are revealed in the EPR or ENDOR spectrum of a defect, important information about the defect such as the distribution of the unpaired electron nearby the defect and the nature of the impurities involved in the defect can be obtained and a microstructural model of the defect may be proposed. The hyperfine interaction is due to the coupling of the magnetic moment of the unpaired electron with a nuclear magnetic moment nearby the defect. In order to calculate the hyperfine interactions we must get the theoretical wave function of the unpaired electron of the defect at first.

Considerable progress has been made in theoretical understanding of electronic structures of defects in semiconductors.¹⁻³ Although the self-consistent Green's-function theories⁴⁻⁶ are capable of producing accurate defect energy levels and wave functions, they typically require very large computer resources. So the empirical non-self-consistent Green's-function methods have also been advanced. The theory of Hjalmanson *et al.*⁷ is one of them. In their theory the central-cell defect potential (CCDP) approximation and the Koster-Slater Green's function method are involved. Their method has been modified to calculate A_1 (T_d point group) (Ref. 8) and T_2 (T_d) (Ref. 9) symmetric deep state wave functions of substitutional defects in covalent semiconductors of diamond or zinc-blende structure. Because the symmetry lowering due to lattice distortion around the defect is not considered in their model, the possible symmetry type of a deep state produced by a substitutional defect is either A_1 (T_d) or T_2 (T_d) under the CCDP approximation.

In fact, the lattice around a defect is subject to distortion in many cases. One important cause for the distortion is the Jahn-Teller effect. Such a distortion occurs when an electron is going to occupy the degenerate state. As a consequence of distortion, the point-group symmetry about the defect is lowered and this can be revealed in EPR experiment. One of the best examples of Jahn-Teller distorted point defects is a single vacancy in Si. An ideal vacancy in Si should have T_d symmetry. In fact, the positively charged vacancy in Si has D_{2d} symmetry and the negatively charged vacancy has C_{2v} symmetry from EPR experiment.¹⁰ In Fig. 1 a one-electron linear combination of atomic orbitals (LCAO) molecular-orbital treatment of the single vacancy in Si given by Watkins¹⁰ illustrates the symmetry lowering due to Jahn-Teller distortion. The electronic structure of a single vacancy in Si has been studied by various authors with various methods.¹¹ However, none of the theoretical papers, to our knowledge, does present a calculation of hyperfine interactions of a distorted vacancy

in many cases. One important cause for the distortion is the Jahn-Teller effect. Such a distortion occurs when an electron is going to occupy the degenerate state. As a consequence of distortion, the point-group symmetry about the defect is lowered and this can be revealed in EPR experiment. One of the best examples of Jahn-Teller distorted point defects is a single vacancy in Si. An ideal vacancy in Si should have T_d symmetry. In fact, the positively charged vacancy in Si has D_{2d} symmetry and the negatively charged vacancy has C_{2v} symmetry from EPR experiment.¹⁰ In Fig. 1 a one-electron linear combination of atomic orbitals (LCAO) molecular-orbital treatment of the single vacancy in Si given by Watkins¹⁰ illustrates the symmetry lowering due to Jahn-Teller distortion. The electronic structure of a single vacancy in Si has been studied by various authors with various methods.¹¹ However, none of the theoretical papers, to our knowledge, does present a calculation of hyperfine interactions of a distorted vacancy

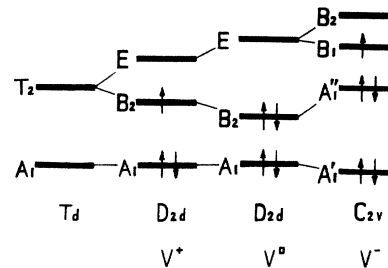


FIG. 1. One-electron molecular orbital treatment for the single vacancy in Si given by Watkins (Ref. 10). The linear combinations of the four broken bonds on the atoms around the vacancy formed the defect molecular orbitals, an A_1 (T_d) singlet and a T_2 (T_d) triplet for an ideal vacancy. The partially degenerate orbitals caused the Jahn-Teller distortions thus lowering the defect symmetry from T_d to D_{2d} and further from D_{2d} to C_{2v} .

(V^+ or V^-) in Si and serves as direct comparison with experimental results of EPR (Ref. 12) or ENDOR.¹³

In the present work we follow the methods provided by Hjalmarsen *et al.*⁷ and Ren *et al.*⁸ for calculating the electronic structure of an unrelaxed substitutional impurity and extend them to calculate the electron wavefunction distribution around the symmetry-lowering single vacancy (V^+ or V^-) in Si. From the calculated wave functions we calculate further the hyperfine interactions for the vacancy and compare our results with EPR or ENDOR data. The main points of this work are the following: (i) to show if and how the empirical tight-binding Green's function method under the CCDP approximation can be used to deal with the electron wave function of a distorted defect; (ii) to show how the extension of the defect potential can be made to the nearest neighbors of the vacancy, and then calculations of electron wave functions can be performed in this case; (iii) to give a quantitative explanation for the first time on the hyperfine interactions from EPR or ENDOR for the single vacancy in Si.

II. CALCULATIONS OF WAVE FUNCTIONS OF DISTORTED SINGLE VACANCY

A. Central-cell defect potential approximation

Let

$$\hat{H}|\psi\rangle = (\hat{H}_0 + \hat{V})|\psi\rangle = E|\psi\rangle \quad (1)$$

be the Schrödinger equation of the imperfect semiconductor containing a lattice vacancy. Here \hat{H}_0 is the one-electron Hamiltonian of the perfect crystal, which is treated with the empirical tight-binding nearest-neighbor approximation of Vogl *et al.*,⁴ and \hat{H} is the one-electron Hamiltonian of the defect-containing crystal. \hat{V} is the defect potential. If there is such a relaxation in the vicinity of the vacancy that the symmetry of \hat{V} is lower than T_d , the vacancy is referred to as a distorted vacancy. From group theory, $|\psi\rangle$ is the state transforming according to a definite irreducible representation l of the symmetry point group of \hat{H} . Hence $|\psi\rangle$ is expanded in a set of bases $|l, R, m\rangle$ (Ref. 8)

$$|\psi^l\rangle = \sum_{R,m} |l, R, m\rangle \langle l, R, m | \psi^l \rangle, \quad (2)$$

where $|l, R, m\rangle$ are orthogonal symmetric combinations of sp^3 hybrid orbitals around the vacancy. l labels the irreducible representation of the state $|\psi^l\rangle$. R indexes the R th shell around the vacancy site, e.g., $R=0$ for the vacancy site and $R=1$ for the shell of the nearest neighbors in this work. m indexes the m th basis of the R th shell transforming according to the l -irreducible representation. In diamond or zinc-blende structure semiconductors the possible symmetries of Jahn-Teller distorted single vacancies are D_{2d} , C_{3v} , or C_{2v} , and the possible symmetry types (irreducible representation l) of deep states produced by these defects are listed in Table I. Because the defect state occupied by an unpaired electron must be a nondegenerate one due to Jahn-Teller effect, only one-dimensional representation l in the

tight-binding expansion of the wave function in Eq. (2) will be considered in this work.

As has been indicated in Fig. 1, the degenerate T_2 (T_d) level of an ideal single vacancy in Si splits due to the perturbation when the lattice around the vacancy is distorted. The splitting is only a few tenths of an electron volt from the experiments.^{10,15} Thus we have a degenerate perturbation problem. We divide the defect potential \hat{V} in Eq. (1) into two parts as

$$\hat{V} = \hat{V}_0 + \Delta\hat{V}, \quad (3)$$

where \hat{V}_0 is the defect potential for an ideal single vacancy with T_d symmetry, and $\Delta\hat{V}$ stands for the perturbation potential with lower symmetry due to the lattice distortion. Considering $\Delta\hat{V}$ as a symmetry-lowering perturbation, the zero-order wave function of the nondegenerate state after the perturbation can be constructed according to the symmetry of the state and may be expressed as Eq. (2). The energy level position after the perturbation has not been calculated in this paper, because $\Delta\hat{V}$ is not known quantitatively. However, the zero-order wave function of the state associated with the distorted defect can be calculated if we know the symmetry of $\Delta\hat{V}$.

Koster-Slater Green's-function technique has been widely used in the calculations of deep-level problems. The fundamental equations for a deep level state in the gap are¹⁻³

$$\det |1 - \hat{G}\hat{V}| = 0, \quad (4)$$

where

$$\hat{G} = (E - \hat{H}_0)^{-1}, \quad (5)$$

and

$$|\psi^l\rangle = \hat{G}\hat{V}|\psi^l\rangle. \quad (6)$$

Under the CCDP approximation, nonzero matrix elements of \hat{V} are only $\langle l, 0, m | \hat{V} | l, 0, m \rangle$ of different l and m . In Ref. 7, l was either A_1 (T_d) or T_2 (T_d) and $m=1$. In this work l will be B_2 (D_{2d}) for V^+ or B_1 (C_{2v}) for V^- in Si and $m=1$. Let

$$V_1 = \langle l, 0, 1 | \hat{V} | l, 0, 1 \rangle. \quad (7)$$

TABLE I. Possible symmetries of the ideal and the Jahn-Teller distorted single vacancies in diamond or zinc-blende semiconductors and the possible symmetry types (irreducible representations) of the states of a distorted single vacancy.

Ideal vacancy	Symmetry		Irreducible representation	
	T_d	A_1	T_2	$A_1 + T_2$
Distorted vacancy	D_{2d}	A_1	$B_2 + E$	$A_1 + B_2 + E$
	C_{3v}	A_1	$A_1 + E$	$2A_1 + E$
	C_{2v}	A_1	$A_1 + B_1 + B_2$	$2A_1 + B_1 + B_2$

The solutions of Eqs. (4) and (6) for the above potential reduce to⁷

$$\langle l,0,1 | \hat{G} | l,0,1 \rangle = V_1^{-1} \quad (8)$$

and⁸

$$\langle l,R,m | \psi' \rangle = \frac{\langle l,R,m | \hat{G} | l,0,1 \rangle}{\langle l,0,1 | \hat{G} | l,0,1 \rangle} \langle l,0,1 | \psi' \rangle, \quad (9)$$

where $\langle l,0,1 | \psi' \rangle$ can be obtained by⁸

$$|\langle l,0,1 | \psi' \rangle|^2 = - \frac{(\langle l,0,1 | \hat{G} | l,0,1 \rangle)^2}{\frac{d}{dE}(\langle l,0,1 | \hat{G} | l,0,1 \rangle)}. \quad (10)$$

In the orbital-removal approximation¹⁶ for a lattice vacancy,

$$\langle l,0,1 | \psi' \rangle = 0. \quad (11)$$

Eqs. (11) and (10) determine the energy level of a single vacancy before the perturbation splitting. This energy level should be equal to the T_2 (T_d) state level of an ideal vacancy, which is 0.51 eV above the valence-band edge in Si.⁹

B. Extended defect potential approximation

From the self-consistent Green's-function work on the single vacancy in Si (Refs. 4 and 5) it has been found that the vacancy potential is short ranged and extends up to the nearest neighbors of the vacancy. The diagonal matrix elements of the defect potential on the nearest neighbors of the vacancy were first introduced by Pecheur *et al.*¹⁷ to respond to different charge states of the vacancy which remained T_d symmetry. In the present study, both the diagonal matrix elements of the defect potential \hat{V} on the nearest neighbors of the distorted vacancy and the off-diagonal matrix element of \hat{V} , which couple the defect to its nearest neighbors, are considered. Such a defect potential is referred to as extended defect potential (EDP) being relative to the CCDP in this paper. By use of the EDP approximation and the empirical tight-binding Green's-function method in the preceding part of this section, the wave function of the distorted vacancy can again be calculated.

We attempt to describe the EDP with the following parameters:

$$V_1 = \langle l,0,1 | \hat{V} | l,0,1 \rangle, \quad (12a)$$

$$W = \langle l,0,1 | \hat{V} | l,1,1 \rangle = \langle l,1,1 | \hat{V} | l,0,1 \rangle, \quad (12b)$$

$$V_2 = \langle l,1,1 | \hat{V} | l,1,1 \rangle, \quad (12c)$$

where $|l,1,1\rangle$ is the symmetric combination of the four nearest sp^3 hybrid orbitals directed to the vacancy site. Only these three nonzero matrix elements of \hat{V} are considered in this work. When $W = V_2 = 0$, we have again the CCDP approximation.

The solution of Eq. (6) for the EDP reduces to

$$\begin{aligned} \langle l,R,m | \psi' \rangle &= \langle l,R,m | \hat{G} | l,0,1 \rangle C_1 \\ &+ \langle l,R,m | \hat{G} | l,1,1 \rangle C_2, \end{aligned} \quad (13a)$$

where

$$C_1 = V_1 \langle l,0,1 | \psi' \rangle + W \langle l,1,1 | \psi' \rangle \quad (13b)$$

and

$$C_2 = W \langle l,0,1 | \psi' \rangle + V_2 \langle l,1,1 | \psi' \rangle. \quad (13c)$$

From Eqs. (11) and (13a) we have

$$\langle l,0,1 | \hat{G} | l,0,1 \rangle C_1 + \langle l,0,1 | \hat{G} | l,1,1 \rangle C_2 = 0. \quad (14)$$

By use of the normalization condition for $|\psi'\rangle$ we obtain

$$\begin{aligned} 1 &= \langle \psi' | \psi' \rangle \\ &= \langle \psi' | \hat{V} \hat{G} \hat{V} | \psi' \rangle \\ &= -C_1^2 \frac{d}{dE} \langle l,0,1 | \hat{G} | l,0,1 \rangle \\ &\quad - 2C_1 C_2 \frac{d}{dE} \langle l,0,1 | \hat{G} | l,1,1 \rangle \\ &\quad - C_2^2 \frac{d}{dE} \langle l,1,1 | \hat{G} | l,1,1 \rangle. \end{aligned} \quad (15)$$

The vacancy level cannot be given theoretically in the EDP approximation because of the uncertainty of V_1 , W , and V_2 . However, the experimental energy level will be used to obtain the wave function. If the energy level of the defect is given, C_1 and C_2 can be determined from Eqs. (14) and (15) and finally $\langle l,R,m | \psi' \rangle$ can be calculated from Eq. (13a).

The above calculated wave functions of the unpaired electron localized near the defect will be used to get hyperfine interactions in the next section.

III. CALCULATION OF HYPERFINE INTERACTION

From the wave function of the unpaired electron, the hyperfine interactions with ^{29}Si nuclei around the defect in Si can be calculated. The general form of hyperfine interaction terms in the spin Hamiltonian for an EPR or ENDOR spectrum is

$$\sum_j \mathbf{S} \cdot \vec{\mathbf{A}}_j \cdot \mathbf{I}_j, \quad (16)$$

where the sum on j goes over all atoms whose nuclei have nuclear spins \mathbf{I}_j around the defect. \mathbf{S} is the spin vector of the unpaired electron. From quantum mechanics the tensor components of $\vec{\mathbf{A}}_j$ in Eq. (16) are given by¹⁸

$$A_{\alpha\beta} = g_e g_n \mu_B \mu_n \left[\frac{8\pi}{3} |\psi(0)|^2 \delta_{\alpha\beta} + \left\langle \frac{3r_\alpha r_\beta}{r^5} - \delta_{\alpha\beta} \frac{1}{r^3} \right\rangle \right], \quad (17)$$

where r_α , $r_\beta = x, y, z$, are the components of the position vector \mathbf{r} from the j th nucleus to the electron. g_e is the g factor of the unpaired electron and g_n is that of the j th nucleus. μ_B is the Bohr magneton and μ_n the nuclear magneton. The term with $|\psi(0)|^2$, the electron probability density at the j th nucleus, is the so-called contact interaction term, which is isotropic. The second term in

Eq. (17) is the dipole-dipole interaction term, which is anisotropic.

The calculated wave function $|\psi^l\rangle$ in the preceding section can be expressed as

$$|\psi^l\rangle = \sum_j (C_{jS}^l |jS\rangle + C_{jP_x}^l |jP_x\rangle + C_{jP_y}^l |jP_y\rangle + C_{jP_z}^l |jP_z\rangle), \quad (18)$$

where $C_{jS}^l = \langle jS | \psi^l \rangle$, $C_{jP_x}^l = \langle jP_x | \psi^l \rangle$, etc. $|jS\rangle$, $|jP_x\rangle$, $|jP_y\rangle$, and $|jP_z\rangle$ are atomic 3S and 3P orbitals of the j th Si atom. It is commonly adopted that only the atomic orbitals centered on the j th atom contribute to \vec{A}_j and the contribution of the other atomic orbitals are neglected. Then we obtain the relationships between all components of \vec{A}_j and the coefficients C_{jS}^l , $C_{jP_x}^l$, $C_{jP_y}^l$, and $C_{jP_z}^l$ from Eqs. (17) and (18):

$$A_{xx} = C_S^2 F_\alpha + (2C_{P_x}^2 - C_{P_y}^2 - C_{P_z}^2) F_\beta, \quad (19a)$$

$$A_{yy} = C_S^2 F_\alpha + (2C_{P_y}^2 - C_{P_x}^2 - C_{P_z}^2) F_\beta, \quad (19b)$$

$$A_{zz} = C_S^2 F_\alpha + (2C_{P_z}^2 - C_{P_x}^2 - C_{P_y}^2) F_\beta, \quad (19c)$$

$$A_{xy} = A_{yx} = 3C_{P_x} C_{P_y} F_\beta, \quad (19d)$$

$$A_{yz} = A_{zy} = 3C_{P_y} C_{P_z} F_\beta, \quad (19e)$$

$$A_{zx} = A_{xz} = 3C_{P_z} C_{P_x} F_\beta, \quad (19f)$$

where

$$F_\alpha = \frac{8\pi}{3} g_e g_n \mu_B \mu_n |\psi_{3S}(0)|^2 \quad (19g)$$

and

$$F_\beta = \frac{2}{5} g_e g_n \mu_B \mu_n \langle r^{-3} \rangle_{3P}. \quad (19h)$$

All suffixes j and l of the coefficients are dropped in Eqs. (19a)–(19f). $|\psi_{3S}(0)|^2$ in Eq. (19g) is the probability density of the 3S orbital of the Si atom at its nucleus site, and $\langle r^{-3} \rangle_{3P}$ in Eq. (19h) is the expectation value of r^{-3} weighted over the 3P orbital of the Si atom. Two groups of values for $|\psi_{3S}(0)|^2$ and $\langle r^{-3} \rangle_{3P}$ have often been used in the literatures on EPR and ENDOR studies of defects in Si: $|\psi_{3S}(0)|^2 = 31.5 \times 10^{24} \text{ cm}^{-3}$ and $\langle r^{-3} \rangle_{3P} = 16.1 \times 10^{24} \text{ cm}^{-3}$ from Ref. 19; $|\psi_{3S}(0)|^2 = 34.5 \times 10^{24} \text{ cm}^{-3}$ and $\langle r^{-3} \rangle_{3P} = 18.2 \times 10^{24} \text{ cm}^{-3}$ from Ref. 20. Because the difference between them is about 10%, the calculating tensor components in Eqs. (19a)–(19f) will also be 10% different with the two groups of values. The latter group is used in this work.

In EPR or ENDOR experiments, each hyperfine tensor is usually reduced to diagonal form by a coordinate transformation to its principal axes. The largest princi-

pal value is taken as A_1 , the second largest as A_2 . New parameters a , b , and c are determined by

$$\vec{A} = \begin{pmatrix} A_1 & 0 & 0 \\ 0 & A_2 & 0 \\ 0 & 0 & A_3 \end{pmatrix} \equiv \begin{pmatrix} a+2b & 0 & 0 \\ 0 & a-b+c & 0 \\ 0 & 0 & a-b-c \end{pmatrix}. \quad (20)$$

Here $a = \frac{1}{3} \text{Tr} \vec{A}$ represents the isotropic part of the hyperfine interaction. b gives the purely axial symmetric part of the hyperfine tensor and c takes account for the deviation from axial symmetry. It has been generally found in EPR and ENDOR experiments that $c \ll b$, i.e., the hyperfine tensor is a nearly axial symmetric tensor, for most point defects.

To compare the theoretical results with the experiments, the hyperfine tensor from Eqs. (19a)–(19f) is reduced to the diagonal form with

$$A_1 = C_S^2 F_\alpha + 2(C_{P_x}^2 + C_{P_y}^2 + C_{P_z}^2) F_\beta, \quad (21a)$$

$$A_2 = A_3 = C_S^2 F_\alpha - (C_{P_x}^2 + C_{P_y}^2 + C_{P_z}^2) F_\beta. \quad (21b)$$

The hyperfine parameters a , b , and c can be obtained by

$$a = C_S^2 F_\alpha, \quad (22a)$$

$$b = (C_{P_x}^2 + C_{P_y}^2 + C_{P_z}^2) F_\beta, \quad (22b)$$

$$c = 0. \quad (22c)$$

The tensor is purely axial symmetric from calculations and the axial direction is determined by the direction cosines which are proportional to C_{P_x} , C_{P_y} , and C_{P_z} , respectively.

If a point defect in diamond or zinc-blende structure semiconductors has a $\{110\}$ mirror plane, two of $|C_{P_x}|$, $|C_{P_y}|$, and $|C_{P_z}|$, when the coordinate directions are along the cubic axes, should be equal to each other for an atom located in the mirror plane. This is the case of the vacancy in Si. Thus the axial direction of the hyperfine tensor is in the mirror plane where the atom is located giving rise to the hyperfine tensor. In this case the axial direction is presented by the angle θ ($0^\circ \leq \theta \leq 90^\circ$) between the axial direction and the $\langle 110 \rangle$ direction in the mirror plane. Suppose $|C_{P_y}| = |C_{P_z}| \neq |C_{P_x}|$, θ can be given by

$$\theta = \arctan \left| \frac{C_{P_x}}{\sqrt{2}C_{P_y}} \right|. \quad (23)$$

IV. RESULTS

A. Positively charged single vacancy V^+ in Si

Let the unpaired electron of V^+ occupy a B_2 (D_{2d}) symmetric state as has been indicated in Fig. 1. Because no ENDOR data for V^+ are available, we calculate the hyperfine interactions arising from the nearest-neighbor atoms and compare them with EPR data.¹² [100] axis is taken to be the cross line of the two {110} mirror planes of V^+ with D_{2d} symmetry. Then the calculated wave function on the nearest-neighbor atom along the [111] direction is given by $C_S=0.1577$, $C_{P_x}=0.2071$, and $C_{P_y}=C_{P_z}=0.1920$ under the CCDP approximation. The wave function on the other three nearest-neighbor atoms can be obtained from the transforming properties of a B_2 (D_{2d}) state. Thus the hyperfine tensors for the four nearest atoms are the very same except for their different axial directions, in agreement with EPR results.¹² The energy level of V^+ is located at 0.13 eV above the valence-band edge from the experiment of Watkins and Troxell.¹⁵ This experimental energy level is needed as input in the calculation under the EDP approximation. Detailed comparison is presented in Table II. As usual η^2 represents probability of the unpaired electron on one atom, i.e., $\eta^2=C_S^2+C_{P_x}^2+C_{P_y}^2+C_{P_z}^2$ and α^2 is the percentage S character of the wave function on the atom which is given by $\alpha^2=C_S^2/\eta^2$. The angle θ for the four nearest-neighbor atoms are the same value. But remember that the axial directions are different for the four atoms while θ is associated with a special $\langle 110 \rangle$ direction which is in the {110} mirror plane containing the corresponding atom. The theoretical results of CCDP calculations coincide with the EPR data quite well and the results of EDP calculations give an even better description of the V^+ defect state especially on α^2 , a , and θ , as can be seen in Table II.

B. Negatively charged single vacancy V^- in Si

From the ENDOR data of V^- in Si, some assignments of hyperfine tensors to lattice positions were given particularly along a $\langle 110 \rangle$ chain of atoms passing through the vacancy site.¹³ Our results of B_1 (C_{2v}) state

TABLE II. Calculated results of wave-function and hyperfine parameters for the nearest-neighbor atoms of V^+ in Si and the EPR data taken from Ref. 12. The CCDP results are in the first line and the EDP results in the second line. θ is 35.3° for $\langle 111 \rangle$ directions.

	η^2 (%)	α^2 (%)	a (MHz)	b (MHz)	c (MHz)	θ (deg)
CCDP	14.7	21.9	146.9	13.2	0	35.6
EDP	14.2	17.6	113.2	13.4	0	37.3
EPR data	14.8	15.1	103.3	14.3	0	42

show that the electron distributes almost only on two of the four nearest-neighbor atoms, $\eta^2=29.5\%$ for each of the two atoms in the symmetric mirror plane of the B_1 (C_{2v}) state and $\eta^2 < 0.1\%$ for the other two atoms from the CCDP approximation results. These results agree well with the ENDOR data (27.3% and 0.6%, respectively), and this confirms again that the unpaired electron of V^- occupies a state of symmetry type B_1 (C_{2v}) as has been proposed by Watkins.^{10,12} On account of the uncertainty of the experimental energy level of V^- in the gap, we have taken the energy level equal to 0.75 eV or 0.90 eV above the valence-band edge in the EDP calculations so as to coincide with experimental η^2 or α^2 separately. The results for some atom sites and the ENDOR data with the assignments from Ref. 13 are shown in Table III. Our results agree well with the ENDOR data only for the nearest-neighbor atoms. In both cases of the EDP calculations ($E_v+0.75$ eV and $E_v+0.90$ eV), closer agreements with the ENDOR data are obtained than those of the CCDP calculations as can be seen in Table III.

V. DISCUSSION AND CONCLUSIONS

(i) We have calculated the hyperfine interactions on the nearest-neighbor atoms of both the positive and negative single vacancies in Si for the first time. Good agreement with experimental data have been obtained even from the CCDP approximation. In order to improve the understanding of the distorted vacancy we have extended the defect potential to the nearest neighbors of the vacancy by the EDP approximation considering both the diagonal and off-diagonal matrix elements of the potential. As for the positive vacancy in Si, the experimental energy level has been used as input in the EDP calculations to obtain the wave function and then the hyperfine tensors. Better agreement has been reached, especially for the fraction S character (α^2), the isotropic part (a), and the axial direction (θ) of the hyperfine tensor. As for the negative vacancy in Si, the energy level, which has not been determined from experiments, was given to fit the experimental result of η^2 or α^2 and then the hyperfine tensors have been calculated. Closer agreement has also been obtained as can be seen in Table III. Thus the EDP approximation produces a better description of both positive and negative vacancies than the CCDP approximation.

The theories of Hjalmarson *et al.*⁷ and Ren *et al.*⁸ for a substitutional impurity in unrelaxed sp^3 -bonded semiconductors have been extended to calculate the electron wave functions of the distorted single vacancies. Considering that the defect symmetry and the irreducible representation according to which the wave function transforms determine the main characters of the wave function, we have calculated just the zero-order wave functions of the degenerate perturbation theory. However, good results of hyperfine tensors have been obtained to be compared with experiments.

The calculating procedure described in this paper can be extended to deal with distorted single vacancies and

TABLE III. Calculated results of wave-function and hyperfine tensor parameters for some atoms in the [011] chain of atoms, which is in the symmetric mirror plane of the B_1 (C_{2v}) state and passing through the vacancy. The ENDOR data are taken from Ref. 13. The energy level of V^- taken in the EDP calculations is denoted in parentheses.

Atom position		η^2 (%)	α^2 (%)	a (MHz)	b (MHz)	c (MHz)	θ (deg)
[111] and $[1\bar{1}\bar{1}]$	CCDP	29.5	21.9	294.7	26.4	0	35.1
	EDP ($E_v + 0.75$ eV)	27.4	25.4	316.6	23.4		
	EDP ($E_v + 0.90$ eV)	25.0	28.1	318.8	20.6	0	35.6
	ENDOR	27.3	28.4	355.8	22.3	1.3	35.2
[022] and $[0\bar{2}\bar{2}]$	CCDP	2.8	0.1	0.1	3.3	0	32.2
	EDP ($E_v + 0.75$ eV)	3.0	0.0	0.0	3.4	0	36.4
	ENDOR	5.9	18.5	50.2	5.5	0.7	35.0
[133] and $[1\bar{3}\bar{3}]$	CCDP	0.5	6.3	1.5	0.6	0	35.2
	EDP ($E_v + 0.75$ eV)	0.3	10.0	1.5	0.3	0	40.7
	ENDOR	3.9	17.1	30.5	3.7	0.3	37.0
[044] and $[0\bar{4}\bar{4}]$	CCDP	0.4	9.2	1.7	0.4	0	31.7
	EDP ($E_v + 0.75$ eV)	0.4	13.0	2.3	0.4	0	35.0
	ENDOR	1.6	18.3	13.5	1.5	0.2	34.8

vacancy complexes in various sp^3 -bonded semiconductors.

(ii) From the EDP calculations we have been able to see the effects of the defect potential's modification. When $W = V_2 = 0$ in Eqs. (13b) and (13c), we have again the CCDP approximation with $C_1 = V_1 \langle l, 0, 1 | \psi^l \rangle$, which can be determined in the CCDP calculations, and $C_2 = 0$. In Table IV, a comparison is given to show the differences between the CCDP and the EDP approximations, where the values of W and V_2 are obtained from Eqs. (13a)–(13c) on the assumption that the value of $V_1 \langle l, 0, 1 | \psi^l \rangle$ is the same as that from the CCDP calculations. As can be seen in Table IV, the changes are 2–4% of C_1 but a remarkable nonzero value of C_2 . It can be also seen that W is not negligible compared to V_2 , especially for the negative vacancy in Si.

(iii) In our calculation of a hyperfine tensor, only the

TABLE IV. The parameters associated with the CCDP and EDP approximations. In the CCDP approximation, W , V_2 , and C_2 all equal zero. The energy level of negative vacancy in Si is taken to be 0.75 eV above the valence-band edge in the EDP approximation.

	CCDP approx.		EDP approx.		
	C_1 (eV)	C_1 (eV)	C_2 (eV)	W (eV)	V_2 (eV)
Positive vacancy	2.472	2.423	-0.494	-0.065	-0.659
Negative vacancy	2.472	2.350	0.303	-0.165	0.409

contributions of the atomic orbitals of the atom to which the hyperfine tensor belongs are considered, so that we have the purely axially symmetric tensor, i.e., $c = 0$. The correction terms coming from the contributions of the other atomic orbitals allow for deviations from axial symmetry.²¹ As can be seen in Table II and III, the experimental values of c are smaller than the values of a and b , i.e., the tensors are nearly axially symmetric. Thus the correction terms are thought to be very small and have been neglected.

(iv) It is particularly worth noticing that the axial direction of a hyperfine tensor is not exactly along a $\langle 111 \rangle$ direction from both experimental and theoretical results. In fact, the axial direction can even be along a $\langle 110 \rangle$ or $\langle 100 \rangle$ direction from experiments.²² Hence, as we compare theoretical results with experimental data, not only the principal values but also the axial directions of hyperfine tensors should be taken as important objects. In fact, the assignments of hyperfine tensors to lattice sites are very difficult in ENDOR studies.²² Thus theoretical calculations of both principal values and axial directions of hyperfine tensors are helpful to the assignments.

(v) We had expected that the EDP approximation would improve the calculated hyperfine tensors of the next nearest neighbor and perhaps the more distant atoms. But the results in Table III show that little improvement has been obtained, particularly for the a value. Thus we should think that the simplification of the defect potential is not the main reason for poor agreement. It should be pointed out that even for an

undistorted substitutional impurity in Si, poor agreements of hyperfine tensors have been obtained for the next nearest neighbor and the more distant atoms.²³ Thus the lattice distortion should not be the main reason for the poor agreements, too.

In fact if only 1% of the unpaired electron were localized on the S orbital of the next-nearest-neighbor atom, from Eq. (22a) where the constant F_α is 4.55×10^3 MHz, one would derive a comparable a value with the ENDOR data. A further study is underway to account for this 1% localization.

(vi) In the ground state of the one-electron model in Fig. 1, the unpaired electron of V^- has the $B_1 (C_{2v})$ symmetric wave function. This implies vanishing of electron localization on the S orbitals of all atoms in the antisymmetric plane of the $B_1 (C_{2v})$ state and then leads to zero a values of the hyperfine tensors belonging to these atoms, in disagreement with the experimental results. From the ENDOR data the largest nonzero a value was 2.1 MHz corresponding to about 0.05% localization on the S orbital of the atom.

In order to overcome the above difficulty, Lannoo²⁴ has considered the influence of many-electron effects in some quantitative detail. He discussed the configuration interaction within the defect molecular model. Considering V^- as a five-electron system and the ground-state configuration as the situation in Fig. 1, there are four excited states with the same symmetry as the ground state. Following his notation the ground state is expressed in the form

$$|\psi_0\rangle = |A'_1 \overline{A'_1} A''_1 \overline{A''_1} B_1\rangle, \quad (24a)$$

where the overbar denotes an electron with opposite spin, and then the four excited states are

$$|\psi_1\rangle = |A'_1 \overline{A'_1} B_2 \overline{B_2} B_1\rangle, \quad (24b)$$

$$|\psi_2\rangle = |A''_1 \overline{A''_1} B_2 \overline{B_2} B_1\rangle, \quad (24c)$$

$$|\psi_3\rangle = |A'_1 \overline{A''_1} B_2 \overline{B_2} B_1\rangle, \quad (24d)$$

$$|\psi_4\rangle = |A''_1 \overline{A'_1} B_2 \overline{B_2} B_1\rangle. \quad (24e)$$

By configuration interaction the excited states are mixed into the ground state. This many-electron effect combined to the coupling between the $A'_1 (C_{2v})$ and $A''_1 (C_{2v})$ states can indeed account for the nonzero a values of the atoms in the antisymmetric plane of the $B_1 (C_{2v})$ state. But a quantitative estimate was arbitrary because it depended sensitively on several uncertain parameters.²⁴

Sprenger *et al.*¹³ proposed that the effect of exchange interaction between the unpaired electron and the closed-shell electrons of the atoms might offer another explanation of the above nonzero a values. Perhaps both effects of configuration interaction and exchange polarization have contributions to the nonzero a values.

From the ENDOR experiment¹³ the nonzero a values in the antisymmetric plane of the $B_1 (C_{2v})$ state are 2 orders smaller than the a value of the nearest-neighbor atom in the symmetric plane of the state. Thus we should think that even if the many-electron effects contribute to the electron localization on the nearest-neighbor atom in the symmetric plane of the state, the contribution is not important. A further study is needed to investigate if the many-electron effects have important contributions to the electron localizations on the next nearest neighbor and more distant atoms.

ACKNOWLEDGMENTS

We thank Professor J. D. Dow and Professor S.-Y. Ren for offering us a computing program of the empirical tight-binding Green's-function method. We are indebted to Professor K. Huang and Professor G. D. Watkins, and also to Mr. L. Long, for helpful discussions. This work was supported in part by the National Science Foundation of China.

¹S. T. Pantelides, *Rev. Mod. Phys.* **50**, 797 (1978).

²M. Lannoo and J. C. Bourgoin, *Point Defects in Semiconductors I. Theoretical Aspects* (Springer, Berlin, 1981).

³M. Jaros, *Deep Levels in Semiconductors* (Hilger, Bristol, 1982).

⁴G. A. Baraff and M. Schlüter, *Phys. Rev. Lett.* **41**, 892 (1978); *Phys. Rev. B* **19**, 4965 (1979).

⁵J. Bernholc, N. O. Lipari, and S. T. Pantelides, *Phys. Rev. Lett.* **41**, 895 (1978); *Phys. Rev. B* **21**, 3545 (1980).

⁶A. Zunger, *Ann. Rev. Mater. Sci.* **15**, 411 (1985).

⁷H. P. Hjalmarson, P. Vogl, D. J. Wolford, and J. D. Dow, *Phys. Rev. Lett.* **44**, 810 (1980).

⁸S.-Y. Ren, W.-M. Hu, O. F. Sankey, and J. D. Dow, *Phys. Rev. B* **26**, 951 (1982); S.-Y. Ren, *Sci. Sin.* **27**, 443 (1984).

⁹M.-F. Li, D.-Q. Mao, and S.-Y. Ren, *Solid State Commun.* **48**, 789 (1983).

¹⁰G. D. Watkins, in *Lattice Defects in Semiconductors 1974*, edited by F. A. Huntley (IOP, London, 1975), p. 1.

¹¹For a detailed list of theoretical papers on the single vacancy in Si, see M. Sprenger, Ph.D. thesis, University of Amsterdam, 1986 (unpublished).

dam, 1986 (unpublished).

¹²G. D. Watkins, in *Radiation Damage in Semiconductors*, edited by P. Baruch (Dunod, Paris, 1965), p. 97.

¹³M. Sprenger, S. H. Muller, and C. A. J. Ammerlaan, *Physica B* **116**, 224 (1983); M. Sprenger, S. H. Muller, E. G. Sieverts, and C. A. J. Ammerlaan, *Phys. Rev. B* **35**, 1566 (1987).

¹⁴P. Vogl, H. P. Hjalmarson, and J. D. Dow, *J. Phys. Chem. Solids* **44**, 365 (1983).

¹⁵G. D. Watkins and J. R. Troxell, *Phys. Rev. Lett.* **44**, 593 (1980).

¹⁶J. Bernholc and S. T. Pantelides, *Phys. Rev. B* **18**, 1780 (1978).

¹⁷P. Pecheur, E. Kauffer, and M. Gerl, in *Defects and Radiation Effects in Semiconductors, 1978*, edited by J. H. Albany (IOP, London, 1979), p. 174.

¹⁸G. D. Watkins, in *Point Defects in Solids*, edited by J. H. Crawford and L. M. Slifkin (Plenum, New York, 1975), Vol. 2, p. 333.

¹⁹G. D. Watkins and J. W. Corbett, *Phys. Rev.* **134**, 1359 (1964).

²⁰J. R. Morton and K. F. Preston, *J. Magn. Resonance* **30**, 577 (1978).

²¹C. A. J. Ammerlaan and J. C. Wolfrat, *Phys. Status Solidi B* **89**, 541 (1978).

²²See, for example, G. W. Ludwig, *Phys. Rev.* **137**, A1520 (1965).

²³Yong-Qiang Jia and Guo-Gang Qin (unpublished).

²⁴M. Lannoo, *Phys. Rev. B* **28**, 2403 (1983).